Temporal and Spatial Variation of PM$_{2.5}$ in Xining, Northeast of the Qinghai–Xizang (Tibet) Plateau

Xiaofeng Hu [1,2,3]**, Yongzheng Yin** [2]**, Lian Duan** [1,3,]*****, Hong Wang** [2]**, Weijun Song** [2] **and Guangli Xiu** [1,2,3,4,]*****

[1] State Environmental Protection Key Laboratory of Risk Assessment and Control on Chemical Processes, East China University of Science and Technology (ECUST), Shanghai 200237, China; xfhu@qhu.edu.cn

[2] Department of Chemical Engineering, Qinghai University, Xining 810016, China; yongzhengyin@qhu.edu.cn (Y.Y.); whong@qhu.edu.cn (H.W.); wjsong@qhu.edu.cn (W.S.)

[3] Shanghai Environmental Protection Key Laboratory of Environmental Standard and Risk Management of Chemical Pollutants, East China University of Science and Technology, Shanghai 200237, China

[4] Shanghai Institute of Pollution Control and Ecological Security, Shanghai 200092, China

* Correspondence: duanlian@ecust.edu.cn (L.D.); xiugl@ecust.edu.cn (G.X.)

check for updates

Abstract: PM$_{2.5}$ was sampled from January 2017 to May 2018 at an urban, suburban, industrial, and rural sites in Xining. The annual mean of PM$_{2.5}$ was highest at the urban site and lowest at the rural site, with an average of 51.5 ± 48.9 and 26.4 ± 17.8 μg·m^{-3}, respectively. The average PM$_{2.5}$ concentration of the industrial and suburban sites was 42.8 ± 27.4 and 37.2 ± 23.7 μg·m^{-3}, respectively. All sites except for the rural had concentrations above the ambient air quality standards of China (GB3095-2012). The highest concentration of PM$_{2.5}$ at all sites was observed in winter, followed by spring, autumn, and summer. The concentration of major constituents showed statistically significant seasonal and spatial variation. The highest concentrations of organic carbon (OC), elemental carbon (EC), water-soluble organic carbon (WSOC), and water-soluble inorganic ions (WSIIs) were found at the urban site in winter. The average concentration of F$^-$ was higher than that in many studies, especially at the industrial site where the annual average concentration of F$^-$ was 1.5 ± 1.7 μg·m^{-3}. The range of sulfur oxidation ratio (SOR) was 0.1–0.18 and nitrogen oxidation ratio (NOR) was 0.02–0.1 in Xining. The higher SO$_4^{2-}$/NO$_3^-$ indicates that coal combustion has greater impact than vehicle emissions. The results of the potential source contribution function (PSCF) suggest that air mass from middle- and large-scale transport from the western areas of Xining have contributed to the higher level of PM$_{2.5}$. On the basis of the positive matrix factorization (PMF) model, it was found that aerosols from salt lakes and dust were the main sources of PM$_{2.5}$ in Xining, accounting for 26.3% of aerosol total mass. During the sandstorms, the concentration of PM$_{2.5}$ increased sharply, and the concentrations of Na$^+$, Ca^{2+} and Mg^{2+} were 1.13–2.70, 1.68–4.41, and 1.15–5.12 times higher, respectively, than annual average concentration, implying that aerosols were mainly from dust and the largest saltwater lake, Qinghai Lake, and many other salt lakes in the province of Qinghai. Time-of-flight secondary ion mass spectrometry (ToF-SIMS) was utilized to study the surface components of PM$_{2.5}$ and F$^-$ was found to be increasingly distributed from the surface to inside the particles. We determined that the extremely high PM$_{2.5}$ concentration appears to be due to an episode of heavy pollution resulting from the combination of sandstorms and the burning of fireworks.

Keywords: carbonaceous components; WSIIs; source apportionment; ToF-SIMS; Xining

1. Introduction

Due to rapid urbanization, industrialization, and economic growth in China, many cities (especially in some developed or industrial areas like northern and eastern China) experience frequent haze

pollution that profoundly impacts visibility, the global climate, and human health [1–5]. Although various actions have been adopted to improve air quality, nearly 70% of 338 cities have $PM_{2.5}$ concentrations well above the national ambient air quality standards (GB3095-2012) [6,7].

The chemical composition of $PM_{2.5}$ is complex, and includes water-soluble inorganic ions (WSIIs), carbonaceous compositions, and mineral components that have significant influence on the physical and chemical properties of aerosols [8–11]. For example, the amount and chemical properties of water-soluble organic carbon (WSOC) can affect the hygroscopic growth and cloud condensation nucleus activity of aerosols [12]. In addition to primary emissions, $PM_{2.5}$ also results from secondary formation, such as through the production of secondary ions (sulfate, nitrate, and ammonium (SNA)) and secondary organic carbon (SOC) [13–15]. The formation mechanism of secondary compositions is highly dependent on the concentration of precursor pollutants, the oxidative state of the atmosphere, and meteorological conditions [16]. In the past few decades, most studies have focused on $PM_{2.5}$ and the relevant haze pollution in developed areas of China such as the Jin-Jing-Ji, Pearl River Delta, and Yangtze River Delta areas [17–20]. Many publications have reported on the haze pollution of western cities such as Xi'an in China, but few have reported on $PM_{2.5}$ in the Qinghai–Tibet Plateau. The Qinghai–Tibet Plateau, also known as the Third Pole [21,22], has significant impact on the global climate [23]. It is not only currently a good site for $PM_{2.5}$, but also for tracing the mixing state of sandstorms and local particles resulting from increasing energy consumption. The lack of oxygen, stronger solar radiation, and lower concentrations of SO_2 and NO_2, undoubtedly influence the composition of $PM_{2.5}$ in Qinghai–Tibet Plateau, but the resulting effects of this remain unclear. A few studies have demonstrated that higher levels of organic aerosols in the plateau environment are oxidized due to the strong solar radiation [24,25].

Xining is the capital city of Qinghai province, and it is located in the northeastern Qinghai–Tibet Plateau [26]. As the largest city in this region with a population of two million, Xining has recently encountered high levels of fine particles due to increasing industrialization. Previous studies have mostly focused on metropoles or cities in developed areas while there are few comprehensive studies on cities of Qinghai–Tibet Plateau. In this study, we conducted a one-year field campaign in which chemical components, including WSIIs and carbonaceous compounds in $PM_{2.5}$, were analyzed at an urban, suburban, industrial, and rural sites in Xining. The main objectives of this study were to (1) characterize the seasonal and spatial variations of $PM_{2.5}$, (2) explore the potential sources of $PM_{2.5}$ on the basis of the potential source contribution function (PSCF) and positive matrix factorization (PMF), and (3) investigate the characteristics of $PM_{2.5}$ on the basis of surface analysis with time-of-flight secondary ion mass spectrometry (ToF-SIMS) during sandstorms. These results help to fill in the gaps in knowledge with regard to $PM_{2.5}$ in the Qinghai–Xizang (Tibet) Plateau.

2. Experimental Methods

2.1. Sampling Sites

$PM_{2.5}$ was sampled at four sites in Xining, an urban, suburban, industrial, and rural site. The details of the four sites are as follows (Figure 1).

The urban site (FPH; N36°37′, E101°46′; 2258 m above sea level) was at Xining First People's Hospital in the urban center of the Chengzhong district, adjacent to Xida Street and Changjiang Road. Therefore, this sampling site is surrounded by both heavy traffic and commercial areas. The air sampler was set on the roof of an outpatient building almost 20 m above ground level.

The industrial site (GID; N36°32′, E101°31″ 2590 m above sea level) was at the Ganhe industrial district, about 36 km southwest away from FPH. The air sampler was about 30 m away from the nearest street, Ganqinger, and set on the top of a building over 10 m above ground level. A variety of industrial activities (such as metal smelting and fertilizer production) are performed in this area.
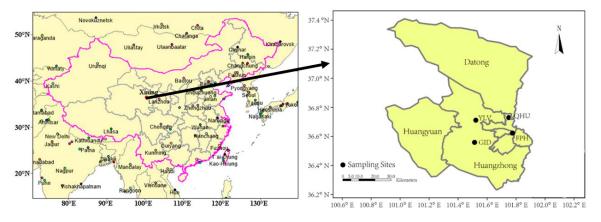
Figure 1. Sampling-site locations.

The suburban site (QHU; N36°43′, E101° 44′; 2330 m above sea level) was at Qinghai University in the northern suburb of Xining, approximately 5 km away from the Science and Technology industrial district and 15 km north of FPH. The air sampler was on the roof of Department of Chemical Engineering building of Qinghai University, approximately 18 m above ground level. The nearest road, Haihu, was almost 50 m away. There was no large industrial source nearby.

The rural site (YLV; N36°42′, E101°31′; 2426 m above sea level) was at the village of Yula, which is northwest of Xining and about 30 km from FHP. This site is representative of rural areas, without any industrial emissions present. The air sampler was set on the roof of a farmer's house, 3 m above ground level.

$PM_{2.5}$ was collected by medium-volume $PM_{2.5}$ samplers (TH-150C China) at a flow rate of 100 L min^{-1}. All filters were 90 mm quartz (Whatman Inc., Maidstone, UK) and prebaked at 600 °C for 4.5 h before sampling. After being stabilized at 20 ± 1°C temperature and 30% ± 2% humidity, filters were weighed before and after sampling with an analytical scale (Mettler Toledo XP205DR, Zurich, Switzerland; precision: 0.01 mg). All filters were individually packed with aluminum foil, sealed in clean plastic bags, and stored at −18 °C until analysis. In total, 311 samples were collected from 7 January 2017 to 28 May 2018. Details are outlined in Table 1.

Table 1. Number of samples at each site per season (2017–2018).

Season	FPH	GID	QHU	YLV
Spring	15	15	38	12
Summer	26	19	15	17
Autumn	16	21	17	13
Winter	37	15	15	20

FPH, First People's Hospital; GID, Ganhe industrial district; QHU, Qinghai University; YLV, Yula village.

2.2. Chemical Analysis

Half of each filter was cut into small pieces and then ultrasonically extracted with 20 mL ultrapure Milli-Q water (18.2 MΩcm^{-1}) for 40 min. Following filtration using a microporous membrane filter (pore size: 0.45 μm), all filtrates were stored at 4 °C in precleaned glass bottles until analysis. Five cations (Na^+, NH_4^+, K^+, Mg^{2+}, and Ca^{2+}) were analyzed using Dionex ICS5000 (Thermo Fisher Scientific, Waltham, USA). Five anions (F^-, Cl^-, NO_3^-, $C_2O_4^{2-}$, and SO_4^{2-}) were analyzed using Dionex ICS1100 (Thermo Fisher Scientific, Waltham, USA). To efficiently separate the ions, a gradient weak base eluent ($KOH + H_2O$) was used for anion detection at a flow rate of 1.5 mL/min. Water-soluble organic carbon (WSOC) was measured with a Multi N/C 2100 (Analytik-Jena, Jena, Germany).

A small piece (0.526 cm^2) was taken from each filter for organic carbon (OC) and elemental carbon (EC) analysis using a carbon analyzer (Desert Research Institute Model 2001) [27]. Detailed procedures

can be found in our previous study [28]. Surface analysis of $PM_{2.5}$ was performed with a ToF-SIMS V instrument (ION-ToF GmbH, Germany). A small punch (10 mm × 8 mm) of each filter was taken to match the sample holder as detailed in our previous study [29]. In this study, we obtained clear images of Na^+, NH_4^+, K^+, Mg^{2+}, and Ca^{2+} by ToF-SIMS, while images of F^-, Cl^-, NO_3^-, $C_2O_4^{2-}$, and SO_4^{2-} were unclear because of a matrix effect, and these images are not shown.

2.3. Air Pollutants and Meteorological Data

The data of SO_2, NO_2, and O_3 were obtained from national air quality monitoring stations (http://www.xnepb.gov.cn/). Temperature (T), relative humidity (RH), wind direction (WD), and wind speed (WS) were collected from the Xining Meteorological Institute (http://qh.cma.gov.cn/).

2.4. Potential Source Contribution Function (PSCF) and Positive Matrix Factorization (PMF)

In this study, the potential source contribution function (PSCF) was applied to identify the potential source regions that contributed to the elevated $PM_{2.5}$ episodes. Positive matrix factorization (PMF) was used for source apportionment in this study. Uncertainties for individual species were $c_{ij} \geq MDL_j$, calculated as (1); $c_{ij} \leq MDL_j$, calculated as Equations (2) and (3).

$$u_{ij} = s_{ij} + 1/3 \times MDL_j \tag{1}$$

$$c_{ij} = 1/2 \times MDL_j \tag{2}$$

$$u_{ij} = 5/6 \times MDL_j, \tag{3}$$

where c_{ij}, u_{ij}, and s_{ij} are the concentration, uncertainty, and analytical uncertainty of species j in the i-th sample, and MDL_j is the method detection limit for species j [30,31]. This method has been previously described in detail in a previous report [32]. The input observable parameters included OC, EC, WSOC, and 7 ions (Na^+, NH_4^+, K^+, Ca^{2+}, Cl^-, NO_3^-, and SO_4^{2-}). In this study, F^-, Mg^{2+}, and $C_2O_4^{2-}$ were excluded due to the low signal-to-noise (S/N) ratios that were acquired.

3. Results and Discussion

3.1. PM$_{2.5}$ and Chemical Compositions

3.1.1. PM$_{2.5}$

The annual average concentration of $PM_{2.5}$ in Xining was 40.6 ± 34.6 μg·m^{-3}; the highest concentration was 51.5 ± 48.9 μg·m^{-3}, observed at FPH, and the lowest in YLV, with an average of 26.4 ± 17.8 μg·m^{-3}. The average $PM_{2.5}$ concentration of GID and QHU was 42.8 ± 27.4 and 37.2 ± 23.7 μg·m^{-3}, respectively. All sites except YLV had concentrations above the ambient air quality standards of China (GB3095-2012). In this study, the determined $PM_{2.5}$ concentrations was lower than the recorded levels for provincial capitals in western China, including Xi'an [33], Lanzhou [34], and Chengdu [35], and much higher than those of studies in the Qinghai–Tibet Plateau [24,36,37].

In addition, the $PM_{2.5}$ concentration also shared similar seasonal variation across sampling sites as those of most studies, being highest in winter and lowest during summer. On the one hand, during winter, coal combustion heating systems can release large amounts of air pollutants. Lower temperature and wind speed in winter can also result in a lower mixing layer, which contributes to particle accumulation. The average $PM_{2.5}$ concentrations in spring were higher than those in autumn at the suburban and rural sites, and quite different from those at the other two sites (FPH and GID). These findings were the opposite of results obtained for Ningbo [38]. This can be ascribed to the following reasons: (1) in the past, straw was burned randomly in autumn, but burning straw in fields is now prohibited by government legislation; and (2) dust is prone to occurring in spring, and YLV and QHU are surrounded by bare fields, which makes them more likely to form dust.

3.1.2. OC/EC

At FPH, OC concentrations ranged from 1.6 to 24.6 $\mu g \cdot m^{-3}$ with an annual average of 9.3 ± 5.5 $\mu g \cdot m^{-3}$, and EC concentrations ranged from 0.3 to 10.8 $\mu g \cdot m^{-3}$ with an annual average of 2.2 ± 2.0 $\mu g \cdot m^{-3}$. At GID, OC ranged from 1.3 to 22.5 $\mu g \cdot m^{-3}$ (average: 6.2 ± 4.4 $\mu g \cdot m^{-3}$), and EC ranged from 0.2 to 5.9 $\mu g \cdot m^{-3}$ (average: 1.6 ± 1.2 $\mu g \cdot m^{-3}$). At QHU, annual average OC concentration was 6.3 ± 5.1 $\mu g \cdot m^{-3}$, and average EC was 1.8 ± 1.0 $\mu g \cdot m^{-3}$. At YLV, the annual average concentration of OC was 6.7 ± 5.0 $\mu g \cdot m^{-3}$, whereas average EC was 2.1 ± 1.0 $\mu g \cdot m^{-3}$. Generally, concentrations of OC and EC in Xining were lower than those in Beijing [39] (25.9 OC and 6.1 $\mu g \cdot m^{-3}$ EC) and Shanghai [40] (14.1 OC and 8.5 $\mu g \cdot m^{-3}$ EC in winter). OC was about four times higher than EC, especially at FPH (6.1 ± 6.0) and GID (7.4 ± 3.9). It is reported that, if OC/EC > 2, secondary organic carbon (SOC) may be formed [41–43]. SOC could be calculated using the following equations:
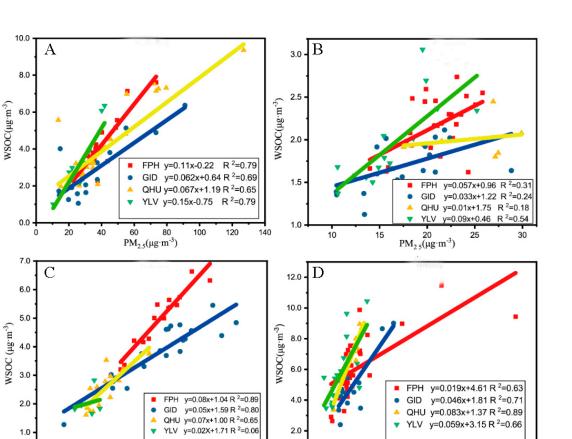
$$POC = EC(OC/EC)_{min} \tag{4}$$

$$OC = OC - POC, \tag{5}$$

where POC is primary organic carbon, and $(OC/EC)_{min}$ is the minimal OC/EC ratio excluding special data for the days when snow, rainstorms, and sandstorms caused drastic changes to the OC/EC ratio during the period of observation [42,44].

SOC concentration at the four sampling sites was highest in winter, which might be attributed to higher levels of gaseous precursor pollutants and the favorable oxidation conditions for secondary conversion in winter. The char-EC/soot-EC ratio is thought to be an indicator for identifying sources from biomass and coal burning or vehicle exhausts [45]. Char-EC is the major constituent of EC and is mainly derived from biomass and coal burning, while soot-EC usually results from vehicle emissions with higher-temperature combustion. According to previous studies, the char-EC/soot-EC of vehicle exhausts is about 0.60, while the char-EC/soot-EC of biomass and coal combustion is about 22.6 [46]. In this study, the average of char-EC/soot-EC shared similar seasonal variation across the sampling sites, with the highest in winter and lowest during summer, the highest average char-EC/soot-EC was 9.6 ± 5.5 at YLV and the lowest average char-EC/soot-EC was 1.3 ± 0.6 at GID in summer, annual average of char-EC/soot-EC at YLV and at GID were 5.1 ± 4.8, 2.8 ± 1.7 indicating that EC was mainly influenced by biomass and coal combustion at YLV, and by vehicle emissions at GID.

3.1.3. WSOC

The annual WSOC concentration in Xining was 4.0 ± 2.0 $\mu g \cdot m^{-3}$, less than that in Beijing [47] and Xi'an, probably due to Xining's smaller population and lower plant coverage than compared to other cities. There was no significant difference in the annual WSOC concentrations at the four sampling sites: GID (3.6 ± 1.6 $\mu g \cdot m^{-3}$) < QHU (3.9 ± 2.1 $\mu g \cdot m^{-3}$) < YLV (4.1 ± 2.3 $\mu g \cdot m^{-3}$) < FPH (4.7 ± 2.1 $\mu g \cdot m^{-3}$). while the seasonal variation of WSOC at the four sampling points were significant statistically (ANOVA, $p < 0.01$). WSOC was highest in the winter and lowest in the summer across all four sites, which might be due to the higher intensity of biomass burning for heating and cooking in winter [48–50]. The annual mean WSOC/$PM_{2.5}$ ratio was 10.7% ± 5.0% across all four sites. The WSOC/$PM_{2.5}$ ratio was highest at YLV (14.2% ± 7.6%) and lowest at FPH (8.8% ± 5.3%). WSOC was more strongly correlated with $PM_{2.5}$ at all four sampling sites in spring, autumn, and winter than in summer (Figure 2). The correlation coefficients of $PM_{2.5}$ and WSOC were higher in winter and lower in summer across the four sampling sites, which can be ascribed to the higher WSOC in winter being formed by the conversion of atmospheric pollutants. WSOC was an important part of $PM_{2.5}$, especially at YLV, because biomass burning is the main source of heating at YLV.

Figure 2. Regressions between water-soluble organic carbon (WSOC) and $PM_{2.5}$ at the four sampling sites. Note: (**A**) = Spring, (**B**) = Summer, (**C**) = Autumn, (**D**) = Winter.

3.1.4. WSIIs
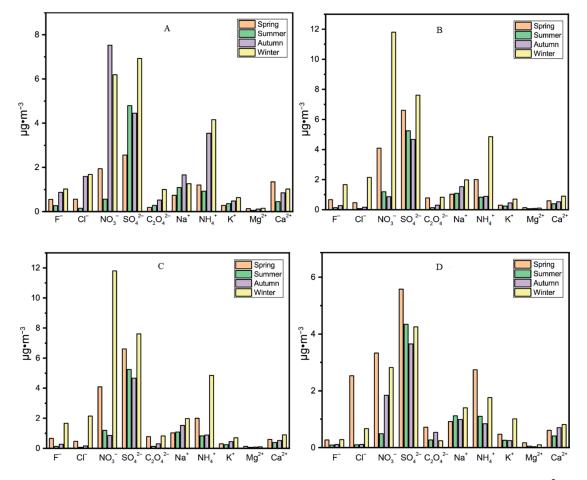
The annual average concentration of total WSIIs was 16.7 ± 10.9 µg·m^{-3}, accounting for $46.1\% \pm 18.2\%$ of $PM_{2.5}$. The annual total WSII concentrations at the four sampling sites showed significant differences statistically (ANOVA, $p < 0.01$), in the following order: YLV (11.7 ± 5.4 µg·m^{-3}) < QHU (16.8 ± 10.2 µg·m^{-3}) < GID (17.1 ± 8.9 µg·m^{-3}) < FPH (20.6 ± 14.5 µg·m^{-3}), contributing to 38.2%–53.8% of $PM_{2.5}$ mass. The ratio of WSIIs to $PM_{2.5}$ at GID was higher than that at YLV, while the opposite pattern was found for the ratio of WSOC to $PM_{2.5}$, which was probably because the sources of YLV were mainly influenced by biomass burning, while those of GID were mainly influenced by industrial emissions.

As shown in Figure 3, WSIIs were highest in winter and lowest in summer across all four sites, and seasonal variations were similar to those in our previous research in Shanghai [51]. In this study, the higher concentrations of Ca^{2+} and Mg^{2+} in spring are mainly due to the frequent occurrence of sand and dust. The concentration of F^- at Xining was higher than that at other Chinese cities [52,53], especially at GID, where the average concentration of F^- was 1.5 ± 1.7 µg·m^{-3}. The high levels of F^- measured in Xining might be associated with material manufacturing, such as electrolytic aluminum and phosphate fertilizer [53,54].

Figure 3. Distribution of water-soluble ions at four sampling sites in Xining, China ($\mu g \cdot m^{-3}$). Note: (**A**) = FPH, (**B**) = GID, (**C**) = QHU, (**D**) = YLV
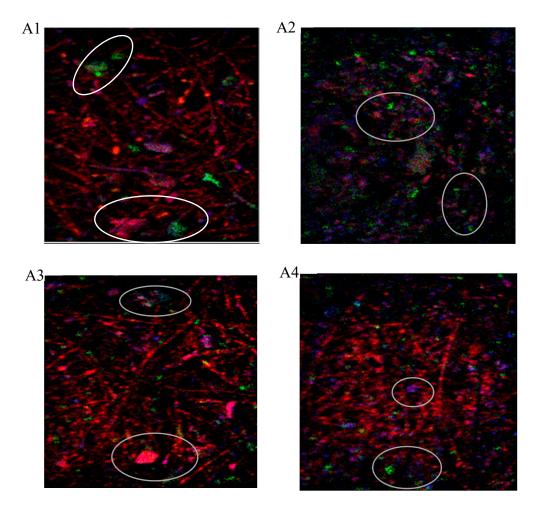
$PM_{2.5}$ mainly originates from external inputs, local emissions, and secondary conversions. The formation and transformation of secondary aerosols are usually characterized by the sulfur oxidation ratio (SOR) and nitrogen oxidation ratio (NOR) [55–57]. SOR and NOR can be calculated using the following equations:

$$SOR = nSO_4^{2-} / \left(nSO_4^{2-} + nSO_2 \right) \tag{6}$$

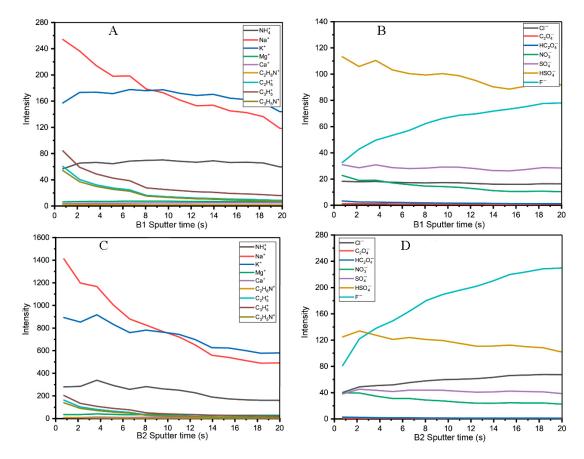$$NOR = nNO_4^{2-} / \left(nNO_4^{2-} + nNO_2 \right) \tag{7}$$

where n is the molar concentration. The range of SOR was 0.1–0.18 and NOR was 0.02–0.1 in Xining. In this study, the highest values for SOR and NOR were observed at FPH in summer and winter, while the lowest SOR and NOR was observed at YLV in autumn and summer, respectively. Results indicated that secondary conversion was more likely to occur at FPH, and the conversion of SO_2 to SO_4^{2-} always occurs in summer, while conversion of NO_2 to NO_3^- was more intensive in winter. High relative humidity and intensive solar radiation in summer could be attributed to the increasing concentrations of SO_4^{2-} [58]. The mass ratio of NO_3^- / SO_4^{2-} was 0.67, suggesting that coal burning had greater impact on $PM_{2.5}$ in Xining than vehicle exhausts, similar to the results in Hangzhou [59].

On the basis of ToF-SIMS, Ca^+, K^+, and Mg^+ were found to be mostly distributed as larger particles at lower concentrations of $PM_{2.5}$ at FPH in Xining, while Ca^+, K^+, and Mg^+ were mostly distributed as smaller particles at higher concentrations of $PM_{2.5}$ relative to the larger particles (Figure 4); the profile was different from our previous research in Shanghai [60], indicating that the formation mechanism and composition of $PM_{2.5}$ in the two cities were different. To explore the sources of

heavy pollution, two samples that were obtained during a pollution episode were selected for depth profiles, which showed that K^+ and the Na^+ signals were stronger than those of other ions (Figure 5). The presence of the two ions gradually decreased going from the surface to the interior particles, with Na^+ decreasing more steeply than K^+. NH_4^+ was more evenly distributed on the surface and interior of particles. Other cations were distributed on the particle surface. SO_4^- was evenly distributed going from the surface to the interior of particles. F^- increased going from the surface to the interior of particles, further research is needed to investigate the mechanism.

Figure 4. Images of $PM_{2.5}$ under positive mode. (**A1,A2**) were low-concentration samples (35.6 and 41.7 µg × m^{-3}), (**A3,A4**) were high-concentration samples (132.6 and 98.4 µg × m^{-3}); relative humidity (RH) on sampling day was 32%, 38%, 35%, and 32%, respectively. Green, fuchsia, and blue represent Ca^+, K^+, and Mg^+, respectively.

Figure 5. Depth profiles for PM$_{2.5}$ samples from FPH in winter. Note: (**A**,**B**) refer to Positive and Negative ions in samples A3, (**C**,**D**) refer to Positive and Negative ions in samples A4.

3.2. PM$_{2.5}$ Source Apportionment in Xining

To exactly identify the spatial distribution of potential sources, the PSCF method was utilized on the basis of the results of backward-trajectory analysis of 72 h air masses. For each day, four trajectories (local time: 2:00, 8:00, 14:00, and 20:00) were employed with an interval of six hours. As shown in Figure 6, most potential source areas with higher PSCF values for PM$_{2.5}$ were located west of Xining, including the Qaidam basin in Qinghai province, the Tarim basin in Xinjiang province, and the Pamirs plateau, where the air mass passed over the desert. Through mid- and large-scale transportation, the air mass that passed over this area made a large contribution to PM$_{2.5}$ concentrations in Xining, the prevailing wind was from west during the sampling period in Xining.

In this study, PMF analysis was conducted to identity emission sources of PM$_{2.5}$ in Xining. PMF input was the dataset (the concentrations of chemical compositions mentioned above) of the PM$_{2.5}$ samples. Samples collected during heavy pollution events, such as sandstorms and the Lunar New year, were excluded. Five to eight factors were tested, and the source profile of the seven-factor solution was the most reasonable. The seven-factor solution was verified to be stable by performing 100 bootstrap runs, as 85% of the runs produced the same factors.

As shown in Figure 7, seven factors associated with the following seven sources were resolved: (1) The main species of Factor 1 were OC (46.5%) and EC (93.6%), which mainly originated from vehicle exhaust [61,62]. The high positive loading of nitrate was 93.2% in Factor 2, which suggested that the secondary conversion of nitrate made major contributions [63]. Factor 3 was characterized by high-loading sodium (61.1%) and potassium (60.8%) that mainly originated from salt lakes [64,65]. Factor 4 was characterized by loading calcium (80.2%) that mainly originate from dust [66,67]. Factor 5 was characterized by loading OC (49.2%) and ammonium (44.1%), which were designated as secondary organic matter [68]. Factor 6 was characterized by loading chloride (93.4%) and potassium

(37.5%), which were designated as combustion sources and industrial emission [69,70]. Factor 7 was characterized by loading sulfate (64.5%) and ammonium (47.3%), which were designated as secondary sulfates [71,72]. Thus, vehicle exhausts (13.8%), secondary nitrate (18.2%), salt lakes (14.6%), dust (11.7%), secondary organic matter (16.1%), combustion sources and industrial emission (12.5%), and secondary sulfate (13.1%) were major PM$_{2.5}$ sources in Xining. Dust mainly comes from transportation, but dust and aerosols from salt lakes were important sources of PM$_{2.5}$ in Xining. Dust and transport from salt lakes were important sources of PM$_{2.5}$ in Xining, this is different from studies in other cities in China [62,63,68,73].
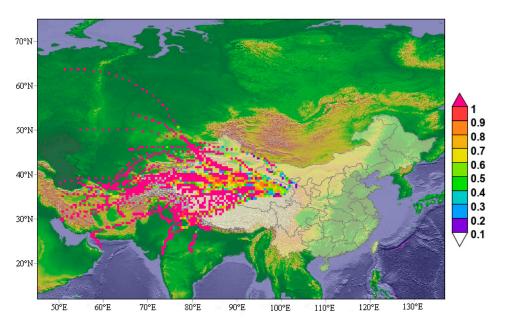

Figure 6. Spatial contribution of PM$_{2.5}$ simulated by potential source contribution function (PSCF) model.
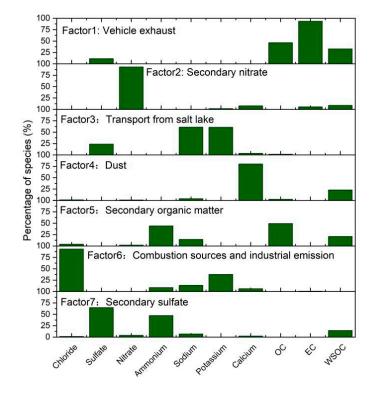

Figure 7. Source apportionment of PM$_{2.5}$ by positive matrix factorization (PMF).

3.3. Special-Pollution-Episode Analysis

3.3.1. Influence of Sandstorms on PM$_{2.5}$

During spring and winter, the frequent occurrence of sand and dust contributed to a higher concentration of PM$_{2.5}$ in Xining. As mentioned above, the dust mainly was from west, FPH located at the most east of Xining. Thus, FPH is the ideal site for investigating the effect of dust in Xining. During the sampling period, there were 10 severely polluted episode affected by sandstorms, particle samples during severely polluted episodes at FPH were chosen to analyze the characteristics of particles. During these sandstorms, the average concentrations of PM$_{2.5}$ and PM$_{10}$ sharply increased, and the concentration of PM$_{2.5}$ reached 1.42–10.21 times higher than the annual average values (Figure 8). The concentrations of Na$^+$, Ca^{2+}, and Mg^{2+} were 1.13–2.70, 1.68–4.41, and 1.15–5.12 times higher than the average concentration, respectively. Na$^+$ mainly comes from marine and industrial emissions, but Xining is an inland city on a plateau; thus, Na$^+$ was likely to come from salt lakes and saltwater lakes such as Qinghai Lake, which is the largest saltwater lake. This is also the reason for the higher concentration of Mg^{2+}. The surface profiles of PM$_{2.5}$ collected at FPH during a sandstorm and a clear day were determined by ToF-SIMS. Particulate matter in the sandstorm greatly increased and almost covered the entire filter area. The silicon fiber on the clean day was very clear, and there were no significant changes in the NH$_4^+$, Ca$^+$, and Mg$^+$ images. K$^+$ and Na$^+$ in the images were more obvious on the clear day. The difference of the negative- and positive-ion spectrum between sandstorm and clear days in Xining was not as obvious as the comparison between haze and clear days in Shanghai [29]. TOF-SIMS was not suitable for analyzing filters polluted by sandstorms, which might be related to the stronger matrix effect caused by the nonconductivity of a large amount of dust.
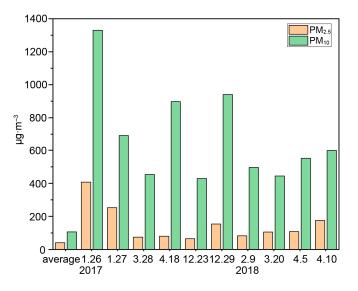

Figure 8. Concentration comparison of PM$_{2.5}$ and PM$_{10}$ between sandstorms and average.

3.3.2. Heavy-Pollution Episode

A severe pollution episode with an AQI of 500 occurred on 26–27 January 2017, where the concentration of PM$_{2.5}$ exceeded 200 μg·m^{-3}. PM$_{2.5}$ concentration peaked at 406.77 μg·m^{-3} on 26 January, which was much higher than the annual average concentration of PM$_{2.5}$. Concentrations of Ca^{2+} and Mg^{2+} increased more sharply than that of Na$^+$ on 26 January. Ca^{2+} and Mg^{2+} are usually thought to be the indicator of dust and sand; thus, the higher levels of PM$_{2.5}$ on 26 January were related to the sandstorm (verified by the Qinghai Meteorological Bureau). Additionally, K$^+$ on 27 January was almost 20 times higher than the annual average value, which is mainly because 27 January was the traditional Chinese New Year's Eve, where a large number of fireworks and firecrackers were burned. On 28 January, high wind speed was helpful for the dilution of air pollutants, so the concentration of

PM$_{2.5}$ decreased. Backward trajectory analysis also demonstrated that the air pollution process was affected by dust from the sandstorm that occurred in the Hexi corridor on 25 January, and the stable weather conditions in Xining contributed to the accumulation of atmospheric pollutants.

4. Conclusions

To comprehensively study the characteristics of WSIIs and organic compositions in addition to the potential sources of PM$_{2.5}$, an over-one-year field measurement study was conducted from January 2017 to May 2018 at four sites in Xining, China: an urban, industrial, suburban, and rural site. The annual mean of PM$_{2.5}$ was the highest at the urban site and lowest at the rural site, with an average of 51.5 ± 48.9 and 26.4 ± 17.8 µg·m^{-3}, respectively. The average PM$_{2.5}$ concentration of the industrial and suburban sites was 42.8 ± 27.4 and 37.2 ± 23.7 µg·m^{-3}, respectively. All sites except the rural had concentrations above the ambient air quality standards of China (GB3095-2012). The highest concentration of PM$_{2.5}$ was observed in winter, followed by spring, autumn, and summer at all sites. The concentration of major constituents of PM$_{2.5}$ showed statistically significant seasonal and spatial variation; the highest concentrations of OC, EC, WSOC, and WSIIs were found in winter at the urban site. The average concentration of F$^-$ was higher than that of many studies in other cities of China, especially at the industrial site, where the annual average concentration of F$^-$ was 1.5 ± 1.7 µg·m^{-3}. PSCF results showed that air mass from mid- and large-scale transportation from the western areas of Xining contributed to the higher level of PM$_{2.5}$. On the basis of PMF, aerosols from salt lakes and dust were found to be important sources of PM$_{2.5}$ in Xining, accounting for 26.3% of aerosol total mass. During the sandstorms, the concentration of PM$_{2.5}$ increased sharply, and concentrations of Na$^+$, Ca^{2+}, and Mg^{2+} were 1.13–2.70, 1.68–4.41, and 1.15–5.12 times higher than the annual average concentration, respectively, and were mainly derived from dust and the largest saltwater lake, Qinghai Lake, and many other salt lakes in Qinghai. The surface profiles of PM$_{2.5}$ showed F$^-$ was increasingly distributed from surface to inside of the particles. During the heavy pollution episode, the combination of sandstorms and burning of fireworks contributed to the occurrence of severe pollution and extremely high concentration of PM$_{2.5}$.

Author Contributions: Conceptualization, W.S.; methodology, H.W.; software, Y.Y.; validation, L.D. and X.H.; data curation, X.H.; writing—original draft preparation, X.H.; writing—review and editing, L.D.; project administration, G.X.; and funding acquisition, G.X. All authors have read and agreed to the published version of the manuscript.

References

1. Sun, Y.L.; Zhuang, G.S.; Tang, A.H.; Wang, Y.; An, Z.S. Chemical characteristics of PM$_{2.5}$ and PM$_{10}$ in haze-fog episodes in Beijing. *Environ. Sci. Technol.* **2006**, *40*, 3148–3155. [CrossRef] [PubMed]
2. Andreae, M.O.; Schmid, O.; Yang, H.; Chand, D.; Yu, J.Z.; Zeng, L.M.; Zhang, Y.H. Optical properties and chemical composition of the atmospheric aerosol in urban Guangzhou, China. *Atmos. Environ.* **2008**, *42*, 6335–6350. [CrossRef]
3. WHO. *Global Health Risks: Mortality and Burden of Disease Attributable to Selected Major Risks*; World Health Organization: Geneva, Switzerland, 2009.
4. Chen, R.; Cheng, J.; Lv, J.; Wu, L.; Wu, J. Comparison of chemical compositions in air particulate matter during summer and winter in Beijing, China. *Environ. Geochem. Health* **2017**, *39*, 913–921. [CrossRef] [PubMed]
5. Gautam, S.; Patra, A.K.; Kumar, P. Status and chemical characteristics of ambient PM$_{2.5}$ pollutions in China: A review. *Environ. Dev. Sustain.* **2018**, *21*, 1649–1674. [CrossRef]

6. Qiao, T.; Zhao, M.F.; Xiu, G.L.; Yu, J.Z. Seasonal variations of water soluble composition (WSOC, Hulis and WSIIs) in PM$_1$, and its implications on haze pollution in urban Shanghai, China. *Atmos. Environ.* **2015**, *123*, 306–314. [CrossRef]

7. Ye, W.F.; Ma, Z.Y.; Ha, X.Z. Spatial–temporal patterns of PM$_{2.5}$ concentrations for 338 Chinese Cities. *Sci. Total Environ.* **2018**, *631–632*, 524–533. [CrossRef]

8. Gao, J.J.; Tian, H.Z.; Cheng, K.; Lu, L.; Zheng, M.; Wang, S.X.; Hao, J.M.; Wang, K.; Hua, S.B.; Zhu, C.Y.; et al. The variation of chemical characteristics of PM$_{2.5}$, and PM$_{10}$, and formation causes during two haze pollution events in urban Beijing, China. *Atmos. Environ.* **2015**, *107*, 1–8. [CrossRef]

9. Liu, J.; Wu, D.; Fan, S.J.; Mao, X.; Chen, H.Z. A one-year, on-line, multi-site observational study on water-soluble inorganic ions in PM$_{2.5}$ over the Pearl River Delta region, China. *Sci. Total Environ.* **2017**, *601–602*, 1720–1732. [CrossRef]

10. He, L.; Chen, H.; Rangognio, J.; Yahyaoui, A.; Colin, P.; Wang, J.H.; Daele, V.; Mellouki, A. Fine particles at a background site in Central France: Chemical compositions, seasonal variations and pollution events. *Sci. Total Environ.* **2018**, *612*, 1159–1170. [CrossRef]

11. Cheng, H.R.; Zhang, F.; Wang, Z.W.; Lv, X.P.; Zhu, Z.M.; Zhang, G.; Wang, X.M. Fine particles (PM$_{2.5}$) at a CAWNET background site in Central China: Chemical compositions, seasonal variations and regional pollution events. *Atmos. Environ.* **2014**, *86*, 193–202. [CrossRef]

12. Alves, C.; Oliveira, T.; Pio, C.; Silvestre, A.J.D.; Fialho, P.; Barata, F.; Legrand, M. Characterisation of carbonaceous aerosols from the Azorean Island of Terceira. *Atmos. Environ.* **2007**, *41*, 1359–1373. [CrossRef]

13. Zhang, Y.Y.; Lang, J.L.; Cheng, S.Y.; Li, S.Y.; Zhou, Y.; Chen, D.S.; Zhang, H.Y.; Wang, H.Y. Chemical composition and sources of PM$_1$ and PM$_{2.5}$ in Beijing in autumn. *Sci. Total Environ.* **2018**, *630*, 72–82. [CrossRef] [PubMed]

14. Hu, G.Y.; Zhang, Y.M.; Sun, J.Y.; Zang, L.M.; Shen, X.J.; Lin, W.L.; Yang, Y. Variability, formation and acidity of water-soluble ions in PM$_{2.5}$, in Beijing based on the semi-continuous observations. *Atmos. Res.* **2014**, *145–146*, 1–11. [CrossRef]

15. Tao, J.; Cheng, T.T.; Zhang, R.J.; Cao, J.J.; Zhu, L.H.; Wang, Q.Y.; Luo, L.; Zhang, L.M. Chemical Composition of PM$_{2.5}$ at an Urban Site of Chengdu in Southwestern China. *Adv. Atmos. Sci.* **2013**, *30*, 1070–1084. [CrossRef]

16. Wang, L.; Ji, D.S.; Li, Y.; Gao, M.; Tian, S.L.; Wen, T.X.; Liu, Z.R.; Wang, L.L.; Peng, X.; Jiang, C.S.; et al. The impact of relative humidity on the size distribution and chemical processes of major water-soluble inorganic ions in the megacity of Chongqing, China. *Atmos. Res.* **2017**, *192*, 19–29. [CrossRef]

17. An, J.; Duan, Q.; Wang, H.; Miao, Q.; Shao, P.; Wang, J.; Zou, J. Fine particulate pollution in the Nanjing northern suburb during summer: Composition and sources. *Environ. Monit. Assess.* **2015**, *187*, 1–14. [CrossRef]

18. Jansen, R.C.; Shi, Y.; Chen, J.M.; Hu, Y.J.; Xu, C.; Hong, S.M.; Li, J.; Zhang, M. Using hourly measurements to explore the role of secondary inorganic aerosol in PM$_{2.5}$ during haze and fog in Hangzhou, China. *Adv. Atmos. Sci.* **2014**, *31*, 1427–1434. [CrossRef]

19. Wang, X.H.; Bi, X.H.; Sheng, G.Y.; Fu, J.M. Chemical composition and sources of PM$_{10}$ and PM$_{2.5}$ aerosols in Guangzhou, China. *Environ. Monit. Assess.* **2006**, *119*, 425–439. [CrossRef]

20. Yao, X.; Chan, C.K.; Fang, M.; Cadle, S.; Chan, T.; Wulawa, P.; He, K.B.; Ye, B.M. The water-soluble ionic composition of PM$_{2.5}$ in Shanghai and Beijing, China. *Atmos. Environ.* **2002**, *36*, 4223–4234. [CrossRef]

21. Wu, J.; Lu, J.; Min, X.Y.; Zhang, Z.H. Distribution and health risks of aerosol black carbon in a representative city of the Qinghai–Tibet Plateau. *Environ. Sci. Pollut. Res.* **2018**, *25*, 19403–19412. [CrossRef]

22. Tripathee, L.; Kang, S.C.; Rupakheti, D.; Zhang, Q.G.; Huang, J.; Sillanpää, M. Water-soluble ionic composition of aerosols at urban location in the foothills of Himalaya, Pokhara Valley, Nepal. *Atmosphere* **2016**, *7*, 102. [CrossRef]

23. Li, R.; Chi, X.L. Thermal comfort and tourism climate changes in the Qinghai–Tibet Plateau in the last 50 years. *Theor. Appl. Climatol.* **2014**, *117*, 613–624. [CrossRef]

24. Meng, J.J.; Wang, G.H.; Li, J.J.; Cheng, C.L.; Cao, J.J. Atmospheric oxalic acid and related secondary organic aerosols in Qinghai Lake, a continental background site in Tibet Plateau. *Atmos. Environ.* **2013**, *79*, 582–589. [CrossRef]

25. Guo, W.; Zhang, Z.Y.; Zheng, N.J.; Li Luo, L.; Xiao, H.Y.; Xiao, H.W. Chemical characterization and source analysis of water-soluble inorganic ions in $PM_{2.5}$ from a plateau city of Kunming at different seasons. *Atmos. Res.* **2020**, *234*, 104687. [CrossRef]

26. Fu, S.X.; Cheng, H.; Qi, C.K. Microarray analysis of gene expression in seeds of Brassica napus planted in Nanjing (altitude: 8.9 m), Xining (altitude: 2261.2 m) and Lhasa (altitude: 3658 m) with different oil content. *Mol. Biol. Rep.* **2009**, *36*, 2375–2386. [CrossRef]

27. Chow, J.C.; Watson, J.G.; Chen, L.W.; Chang, M.C.; Robinson, N.F.; Trimble, D.; Kohl, S. The IMPROVE-A temperature protocol for thermal/optical carbon analysis: Maintaining consistency with a long-term database. *J. Air Waste Manag. Assoc.* **2007**, *57*, 1014–1023. [CrossRef]

28. Duan, L.; Xiu, G.L.; Feng, L.; Cheng, N.; Wang, C.G. The mercury species and their association with carbonaceous compositions, bromine and iodine in $PM_{2.5}$ in Shanghai. *Chemosphere* **2016**, *146*, 263–271. [CrossRef]

29. Huang, D.; Xiu, G.L.; Li, M.; Hua, X.; Long, Y.T. Surface components of $PM_{2.5}$ during clear and hazy days in Shanghai by ToF-SIMS. *Atmos. Environ.* **2017**, *148*, 175–181. [CrossRef]

30. Reff, A.; Eberly, S.I.; Bhave, P.V. Receptor modeling of ambient particulate matter data using positive matrix factorization: Review of existing methods. *Air Waste Manag.* **2007**, *57*, 146–154. [CrossRef]

31. Kuang, B.Y.; Lin, P.; Huang, X.H.H.; Yu, J.Z. Sources of humic-like substances in the Pearl River Delta, China: Positive matrix factorization analysis of PM2.5 major components and source markers. *Atmos. Chem. Phys.* **2015**, *15*, 1995–2008. [CrossRef]

32. Manousakas, M.; Papaefthymiou, H.; Diapouli, E.; Migliori, A.; Karydas, A.G.; Bogdanovic-Radovic, I.; Eleftheriadis, K. Assessment of $PM_{2.5}$ sources and their corresponding level of uncertainty in a coastal urban area using EPA PMF 5.0 enhanced diagnostics. *Sci. Total Environ.* **2017**, *574*, 155–164. [CrossRef] [PubMed]

33. Wang, P.; Cao, J.J.; Shen, Z.X.; Han, Y.M.; Lee, S.C.; Huang, Y.; Zhu, C.S.; Wang, Q.Y.; Xu, H.M.; Huang, R.J. Spatial and seasonal variations of $PM_{2.5}$ mass and species during 2010 in Xi'an, China. *Sci. Total Environ.* **2015**, *508*, 477–487. [CrossRef] [PubMed]

34. Tan, J.H.; Zhang, L.M.; Zhou, X.M.; Duan, J.C.; Li, Y.; Hu, J.N.; He, K.B. Chemical characteristics and source apportionment of $PM_{2.5}$ in Lanzhou, China. *Sci. Total Environ.* **2017**, *601–602*, 1743–1752. [CrossRef] [PubMed]

35. Liao, T.T.; Wang, S.; Ai, J.; Gui, K.; Duan, B.L.; Zhao, Q.; Zhang, X.; Jiang, W.T.; Sun, Y. Heavy pollution episodes, transport pathways and potential sources of $PM_{2.5}$ during the winter of 2013 in Chengdu (China). *Sci. Total Environ.* **2017**, *584–585*, 1056–1065. [CrossRef]

36. Li, C.L.; Chen, P.F.; Kang, S.C.; Yan, F.P.; Hu, Z.F.; Qu, B.; Sillanpaa, M. Concentrations and light absorption characteristics of carbonaceous aerosol in $PM_{2.5}$ and PM_{10} of Lhasa city, the Tibetan Plateau. *Atmos. Environ.* **2016**, *127*, 340–346. [CrossRef]

37. Xu, J.Z.; Zhang, Q.; Wang, Z.B.; Yu, G.M.; Ge, X.L.; Qin, X. Chemical composition and size distribution of summertime $PM_{2.5}$ at a high altitude remote location in the northeast of the Qinghai–Xizang (Tibet) Plateau: Insights into aerosol sources and processing in free troposphere. *Atmos. Chem. Phys.* **2015**, *15*, 5069–5081. [CrossRef]

38. Hou, X.W.; Fei, D.D.; Kang, H.Q.; Zhang, Y.L.; Gao, J.H. Seasonal statistical analysis of the impact of meteorological factors on fine particle pollution in China in 2013–2017. *Nat. Hazards* **2018**, *93*, 1–22. [CrossRef]

39. Zhou, J.M.; Zhang, R.J.; Cao, J.J.; Chow, J.C.; Watson, J.G. Carbonaceous and ionic components of atmospheric fine particles in Beijing and their impact on atmospheric visibility. *Aerosol Air Qual. Res.* **2012**, *12*, 492–502. [CrossRef]

40. Zhao, M.F.; Qiao, T.; Huang, Z.S.; Zhu, M.Y.; Xu, W.; Xiu, G.L.; Tao, J.; Lee, S.C. Comparison of ionic and carbonaceous compositions of $PM_{2.5}$ in 2009 and 2012 in shanghai, china. *Sci. Total Environ.* **2015**, *536*, 695–703. [CrossRef]

41. Chow, J.C.; Watson, J.G.; Louie, P.K.K.; Chen, L.W.A.; Sin, D. Comparison of $PM_{2.5}$ carbon measurement methods in Hong Kong, China. *Environ. Pollut.* **2005**, *137*, 334–344. [CrossRef]

42. Castro, L.M.; Pio, C.A.; Harrison, R.M.; Smith, D.J.T. Carbonaceous aerosol in urban and rural European atmospheres: Estimation of secondary organic carbon concentrations. *Atmos. Environ.* **1999**, *33*, 2771–2781. [CrossRef]

43. Feng, J.L.; Li, M.; Zhang, P.; Gong, S.Y.; Zhong, M.; Wu, M.H.; Zheng, M.; Chen, C.H.; Wang, H.L.; Lou, S.R. Investigation of the sources and seasonal variations of secondary organic aerosols in PM$_{2.5}$, in Shanghai with organic tracers. *Atmos. Environ.* **2013**, *79*, 614–622. [CrossRef]

44. Lim, H.J.; Turpin, B.J. Origins of primary and secondary organic aerosol in Atlanta: Results of time-resolved measurements during the Atlanta supersite experiment. *Environ. Sci. Technol.* **2002**, *36*, 4489–4496. [CrossRef] [PubMed]

45. Han, Y.M.; Cao, J.J.; Lee, S.C.; Ho, K.F.; An, Z.S. Different characteristics of char and soot in the atmosphere and their ratio as an indicator for source identification in Xi'an, China. *Atmos. Chem. Phys.* **2010**, *10*, 595–607. [CrossRef]

46. Han, Y.M.; Lee, S.C.; Cao, J.J.; Ho, K.F.; An, Z.S. Spatial distribution and seasonal variation of char-EC and soot-EC in the atmosphere over China. *Atmos. Environ.* **2009**, *43*, 6066–6073. [CrossRef]

47. Ping, X.; Zhou, X.M.; Duan, J.C.; Tan, J.H.; He, K.B.; Yuan, C.; Ma, Y.L.; Zhang, Y.X. Chemical characteristics of water-soluble organic compounds (WSOC) in PM$_{2.5}$ in Beijing, China: 2011–2012. *Atmos. Res.* **2017**, *183*, 104–112.

48. Zhang, G.; Bi, X.; Chan, L.Y.; Wang, X.; Sheng, G.; Fu, J. Size-segregated chemical characteristics of aerosol during haze in an urban area of the Pearl River Delta region, China. *Urban Clim.* **2013**, *4*, 74–84. [CrossRef]

49. Yan, C.Q.; Zheng, M.; Sullivan, A.P.; Bosch, C.; Desyaterik, Y.; Andersson, A.; Li, X.Y.; Guo, X.S.; Zhou, T.; Gustafsson, Ö.; et al. Chemical characteristics and light-absorbing property of water-soluble organic carbon in Beijing: Biomass burning contributions. *Atmos. Environ.* **2015**, *121*, 4–12. [CrossRef]

50. Ye, Z.L.; Li, Q.; Liu, J.S.; Luo, S.P.; Zhou, Q.F.; Bi, C.L.; Ma, S.S.; Chen, Y.F.; Chen, H.; Li, L.; et al. Investigation of submicron aerosol characteristics in Changzhou, China: Composition, source, and comparison with co-collected PM$_{2.5}$. *Chemosphere* **2017**, *183*, 176–185. [CrossRef]

51. Zhao, M.F.; Huang, Z.S.; Qiao, T.; Zhang, Y.K.; Xiu, G.L.; Yu, J.Z. Chemical characterization, the transport pathways and potential sources of PM$_{2.5}$ in Shanghai: Seasonal variations. Science of the Total Environment. *Atmos. Res.* **2015**, *158–159*, 66–78. [CrossRef]

52. Schleicher, N.; Norra, S.; Chai, F.H.; Chen, Y.Z.; Wang, S.L.; Stuben, D. Seasonal trend of water-soluble ions at one TSP and five PM$_{2.5}$ sampling sites in Beijing, China. *Alliance Glob. Sustain. Bookseries* **2010**, *17*, 87–95.

53. Zhou, H.J.; Lü, C.W.; He, J.; Gao, M.S.; Zhao, B.Y.; Ren, L.M.; Zhang, L.J.; Fan, Q.Y.; Liu, T.; He, Z.X.; et al. Stoichiometry of water-soluble ions in PM$_{2.5}$: Application in source apportionment for a typical industrial city in semi-arid region, Northwest China. *Atmos. Res.* **2018**, *204*, 149–160. [CrossRef]

54. Rogula-Kozowska, W.; Klejnowski, K.; Rogula-Kopiec, P.; Mathews, B.; Szopa, S. A study on the seasonal mass closure of ambient fine and coarse dusts in zabrze, poland. *Bull. Environ. Contam. Toxicol.* **2012**, *88*, 722–729. [CrossRef] [PubMed]

55. Gao, X.; Yang, L.X.; Cheng, S.H.; Gao, R.; Zhou, Y.; Xue, L.K.; Shou, Y.P.; Wang, J.; Wang, X.F.; Nie, W.; et al. Semi-continuous measurement of water-soluble ions in PM$_{2.5}$ in Jinan, China: Temporal variations and source apportionments. *Atmos. Environ.* **2011**, *45*, 6048–6056. [CrossRef]

56. Lin, J.J. Characterization of the major chemical species in PM$_{2.5}$ in the Kaohsiung City, Taiwan. *Atmos. Environ.* **2002**, *36*, 1911–1920. [CrossRef]

57. Chen, C.F.; Liang, J.J. Integrated chemical species analysis with source-receptor modeling results to characterize the effects of terrain and monsoon on ambient aerosols in a basin. *Environ. Sci. Pollut. Res.* **2013**, *20*, 2867–2881. [CrossRef]

58. Lv, B.L.; Zhang, B.; Bai, Y.Q. A systematic analysis of PM$_{2.5}$ in Beijing and its sources from 2000 to 2012. *Atmos. Environ.* **2016**, *124*, 98–108. [CrossRef]

59. Cao, J.J.; Shen, Z.X.; Chow, J.C.; Qi, G.W.; Watson, J.G. Seasonal variations and sources of mass and chemical composition for PM$_{10}$ aerosol in Hangzhou, China. *Particuology* **2009**, *7*, 161–168. [CrossRef]

60. Huang, D.; Hua, X.; Xiu, G.L.; Zheng, Y.J.; Yu, X.Y.; Long, Y.T. Secondary ion mass spectrometry: The application in the analysis of atmospheric particulate matter. *Anal. Chim. Acta* **2017**, *989*, 1–14. [CrossRef]

61. Chan, Y.C.; Simpson, R.W.; Mctainsh, G.H.; Vowles, P.D.; Cohen, D.D.; Bailey, G.M. Source apportionment of PM and PM aerosols in Brisbane (Australia) by receptor modelling. *Atmos. Environ.* **1999**, *33*, 3251–3268. [CrossRef]

62. Zhang, W.H.; Liu, B.S.; Zhang, Y.F.; Li, Y.F.; Sun, X.Y.; Gu, Y.; Dai, C.L.; Li, N.; Song, C.B.; Dai, Q.L.; et al. A refined source apportionment study of atmospheric $PM_{2.5}$ during winter heating period in Shijiazhuang, China, using a receptor model coupled with a source-oriented model. *Atmos. Environ.* **2020**, *222*, 117157. [CrossRef]

63. Zhao, Z.P.; Lv, S.; Zhang, Y.H.; Zhao, Q.B.; Shen, L.; Xu, S.; Yu, J.Q.; Hou, J.W.; Jin, C.Y. Characteristics and source apportionment of $PM_{2.5}$ in Jiaxing, china. *Environ. Sci. Pollut. Res.* **2019**, *26*, 7497–7511. [CrossRef] [PubMed]

64. Cesari, D.; Donateo, A.; Conte, M.; Merico, E.; Giangreco, A.; Giangreco, F.; Contini, D. An inter-comparison of $PM_{2.5}$ at urban and urban background sites: Chemical characterization and source apportionment. *Atmos. Res.* **2016**, *174*, 106–119. [CrossRef]

65. Simoneit, B.R.T.; Schauer, J.J.; Nolte, C.G.; Oros, D.R.; Elias, V.O.; Fraser, M.P.; Rogge, W.F.; Cass, G.R. Levoglucosan, a tracer for cellulose in biomass burning and atmospheric particles. *Atmos Environ.* **1999**, *33*, 173–182. [CrossRef]

66. Xue, Y.H.; Wu, J.H.; Feng, Y.C.; Dai, L.; Bi, X.H.; Li, X.; Zhu, T.; Tang, S.B.; Chen, M.F. Source characterization and apportionment of PM_{10} in Panzhihua, China. *Aerosol Air Qual. Res.* **2010**, *10*, 367–377. [CrossRef]

67. Zhang, R.; Jing, J.; Tao, J.; Hsu, S.C.; Wang, G.; Cao, J.; Lee, C.S.L.; Zhu, L.; Chen, Z.; Zhao, Y.; et al. Chemical characterization and source apportionment of $PM_{2.5}$ in Beijing: Seasonal perspective. *Atmos. Chem. Phys.* **2013**, *13*, 7053–7074. [CrossRef]

68. Li, Y.F.; Liu, B.S.; Xue, Z.G.; Zhang, Y.F.; Sun, X.Y.; Song, C.B.; Dai, Q.L.; Fu, R.C.; Tai, Y.G.; Gao, J.Y.; et al. Chemical characteristics and source apportionment of $PM_{2.5}$ using PMF modelling coupled with 1-hr resolution online air pollutant dataset for Linfen, China. *Environ. Pollut.* **2020**, *263*, 114532. [CrossRef]

69. Xiu, G.L.; Zhang, D.N.; Chen, J.Z.; Huang, X.J.; Chen, Z.X.; Guo, H.L.; Pan, J.F. Characterization of major water-soluble inorganic ions in size fractionated particulate matters in Shanghai campus ambient air. *Atmos. Environ.* **2004**, *38*, 227–236. [CrossRef]

70. Park, E.H.; Heo, J.; Kim, H.; Yi, S.-M. Long term trends of chemical constituents and source contributions of $PM_{2.5}$ in Seoul. *Chemosphere* **2020**, *251*, 126371. [CrossRef]

71. Stockwell, W.R.; Kuhns, H.; Etyemezian, V.; Green, M.C.; Chow, J.C.; Watson, J.G. The treasure valley secondary aerosol study ii: Modeling of the formation of inorganic secondary aerosols and precursors for southwestern Idaho. *Atmos. Environ.* **2003**, *37*, 525–534. [CrossRef]

72. Tian, Y.Z.; Zhang, Y.F.; Liang, Y.L.; Niu, Z.B.; Xue, Q.Q.; Feng, Y.C. $PM_{2.5}$ source apportionment during severe haze episodes in a Chinese megacity based on a 5-month period by using hourly species measurements: Explore how to better conduct PMF during haze episodes. *Atmos. Environ.* **2020**, *224*, 117364. [CrossRef]

73. Qiao, T.; Zhao, M.F.; Xiu, G.L.; Yu, J.Z. Simultaneous monitoring and compositions analysis of PM_1 and $PM_{2.5}$ in shanghai: Implications for characterization of haze pollution and source apportionment. *Sci. Total Environ.* **2016**, *557–558*, 386–394. [CrossRef] [PubMed]